Single-Step Fabrication of Transparent Superhydrophobic Porous Polymer Films

Hiroshi Yabu[†,‡] and Masatsugu Shimomura*[,†,‡,§]

Nanotechnology Research Center, Research Institute for Electronic Science, Hokkaido University, N21W10, Sapporo 001-0021, Japan, Frontier Research System, Institute of Physical and Chemical Research (RIKEN Institute), 1-12, Hirosawa, Wako, Saitama 351-0198, Japan, and Core Research for Evolutional Science and Technology (CREST), Japan Science and Technology Agency (JST), 4-1-8, Honmachi, Kawaguchi, Saitama 332-0012, Japan

Received June 14, 2005
Revised Manuscript Received September 11, 2005

Water repellency is very useful for applications such as dust-free coatings, coverings to prevent snow sticking, and others.[1] Water repellency is dominated by the topology and chemistry of surfaces. For a flat surface, theoretical calculation shows that densely packed CF_3 groups would give the highest water contact angle possible, 120°.[2] In nature, however, superhydrophobic surfaces have been found with water contact angles higher than 120°. Lotus leaf, for example, secretes waxy compounds on its rough surface, which is covered in many small bumps.[3] The water repellency of plant leaves is due to this surface roughness enhancing the hydrophobicity. The water contact angle of the rough surface, θ_w, is described by Wenzel's equation,[4]

$$\cos \theta_w = r \cos \theta$$

where r is the roughness factor and θ is the contact angle for a flat surface. The roughness factor, r, is the ratio of the actual surface area to the apparent surface area of the substrate. The superficial contact angle of a surface composed of two components (e.g., air and polymer) is also given by a formula reported by Cassie[5] based on the fraction of each component's surface area. According to Cassie's law,

$$\cos \theta_c = \phi_1 \cos \theta_1 + \phi_2 \cos \theta_2$$

where θ_c is the superficial contact angle; θ_1 and θ_2 are contact angles of flat films of components 1 and 2, respectively; and ϕ_1 and ϕ_2 are surface area fractions of polymer and air, respectively. Rough or microstructured surfaces are required to form the surface with contact angles of water higher than 150°.[6−12]

For superhydrophobic surface applications such as optical coatings for window glass or painted surfaces, optical transparency is also important. Microstructured surfaces are, however, not transparent due to Mie scattering[13] from their rough surfaces. In the case of the surface structures larger than the visible light wavelength, the Mie scattering has occurred. In this case, the wide range of irradiated light is scattered by the structured surface depending on the size of surface structures, incident angles of light irradiation, and differences of refractive indices between the air and materials. As the result, the structured surface looks opaque. To achieve optical transparency, the size of the underlying structure should be smaller than the wavelength of visible light (at least <400 nm). Therefore, a transparent and superhydrophobic surface requires a highly rough surface on the subwavelength scale. Some papers reported the preparation of a transparent superhydrohophobic surface by preparing a small roughness onto inorganic oxides.[14]

Honeycomb-like microporous polymer films with 500 nm to 50 μm pores (diameter) have been prepared by casting polymer solutions under humid conditions.[15−18] Using this method, we have prepared honeycomb-patterned polymer films as potential functional materials including engineering (e.g., polystyrene) and super-engineering plastics (e.g., polyimide),[19] biodegradable polymers,[20] and titanium oxide.[21] Recently, we have reported that the honeycomb-patterned

* To whom correspondence should be addressed. Tel. & fax: +81-11-706-9369. E-mail: yabu@poly.es.hokudai.ac.jp.
† Hokkaido University.
‡ Institute of Physical and Chemical Research (RIKEN Institute).
§ Japan Science and Technology Agency (JST).

(1) Ball, P. *Nature* **1999**, *400*, 507.
(2) Hozumi, A.; Takai, O. *Thin Solid Films* **1997**, *303*, 222−225.
(3) (a) Barthlott, W.; Neinhuis, C. *Planta* **1997**, *202*, 1, (b) Otten, A.; Herminghaus, S. *Langmuir* **2004**, *20* (6), 2405.
(4) Wenzel, R. N. *Ind. Eng. Chem.* **1949**, *28*, 988.
(5) Cassie, A. B. D. *Discuss Faraday Soc.* **1948**, *3*, 11.
(6) Tada, H.; Nagayama, H. *Langmuir* **1995**, *11* (1), 136.
(7) Öner, D.; McCarthy, T. J. *Langmuir* **2000**, *16* (20), 7777.
(8) (a) Onda, T.; Shibuichi, S.; Satoh, N.; Tsujii, K. *Langmuir* **1996**, *12*, 2125−2127. (b) Tsujii, K.; Yamamoto, T.; Onda, T.; Shibuichi, S. *Angew. Chem., Int. Ed. Engl.* **1997**, *36*, 1011−1012. (c) Shibuichi, S.; Yamamoto, T.; Onda, T.; Tsujii, K. *J. Colloid Interface Sci.* **1998**, *208*, 287−294.
(9) (a) Miwa, M.; Nakajima, A.; Fujishima, A.; Hashimoto, K.; Watanabe, T. *Langmuir* **2000**, *16*, 5754−5760. (b) Nakajima, A.; Hashimoto, K.; Watanabe, T. *Monatsh. Chem.* **2001**, *132*, 31−41.
(10) Wang, R.; Hashimoto, K.; Fujishima, A.; Chikuni, M.; Kojima, E.; Kitamura, A.; Shimohigoshi, M.; Watanabe, T. *Nature* **1997**, *388*, 431−432.
(11) Bico, J.; Marzolin, C.; Quere, D. *Europhys. Lett.* **1999**, *47*, 220−226.
(12) (a) Feng, L.; Li, S.-H.; Li, H.-J.; Zhai, J.; Song, Y.-L.; Jiang, L.; Zhu, D.-B. *Angew. Chem., Int. Ed.* **2002**, *41*, 1221. (b) Feng, L.; Li, S.-H.; Li, Y.-S.; Li, H.-J.; Zhang, L.-J.; Zhai, J.; Song, Y.-L.; Liu, B.-Q.; Jiang, L.; Zhu, D.-B. *Adv. Mater.* **2002**, *14*, 1857−1860. (c) Feng, L.; et al. *Angew. Chem., Int. Ed.* **2003**, *42*, 800−802. (d) Feng, L.; Song, Y.-L.; Zhai, J.; Liu, B.-Q.; Xu, J.; Jiang, L.; Zhu, D.-B. *Angew. Chem., Int. Ed.* **2003**, *42*, 4217−4220.
(13) Mie, G. *Ann. Phys.* **1908**, *25*, 377.
(14) (a) Nakajima, A.; Fujishima, A.; Hashimoto, K.; Watanabe, T. *Adv. Mater.* **1999**, *11*, 1365−1368, (b) Nakajima, A.; Hashimoto, K.; Watanabe, T.; Takai, K.; Yamauchi, A.; Fujishima, A. *Langmuir* **2000**, *16* (17), 7044.
(15) (a) Widawski, G.; Rawiso, M.; Françios, B. *Nature* **1994**, *369*, 387−389. (b) François, B.; Pitois, O.; Francois, J. *Adv. Mater.* **1995**, *7*, 1041.
(16) Govor, L.; Bashmakov, I.; Kiebooms, R.; Dyakonov, V.; Parisi, J. *Adv. Mater.* **2001**, *13*, 588. Stenzel, M. *Aust. J. Chem.* **2002**, *55*, 239−243.
(17) Maruyama, N.; Koito, T.; Nishida, J.; Sawadaishi, T.; Cieren, X.; Ijiro, K.; Karthaus, O.; Shimomura, M. *Thin Solid Films* **1998**, *327−329*, 854.
(18) Karthaus, O.; Maruyama, N.; Cieren, X.; Shimomura, M.; Hasegawa, H.; Hashimoto, T.; *Langmuir* **2000**, *16*, 6071−6076.
(19) (a) Yabu, H.; Tanaka, M.; Ijiro, K.; Shimomura, M. *Langmuir* **2003**, *19*, 6297−6300. (b) Yabu, H.; Shimomura, M. *Langmuir* **2005**, *21* (5), 1709.
(20) Nishikawa, T.; Ookura, R.; Nishida, J.; Arai, K.; Hayashi, J.; Kurono, N.; Sawadaishi, T.; Hara, M.; Shimomura, M. *Langmuir* **2002**, *18*, 5734−5740.

10.1021/cm051281i CCC: $30.25
Published on Web 09/27/2005

Chart 1

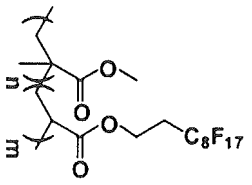

films of fluorinated polymers show superhydrophobicity.[22] However, the films formed were not transparent because the pore size was larger than 1 μm. In the present report we have succeeded in reducing the pore size of honeycomb-patterned fluorinated polymer films to below sub-wavelength. Scanning electron microscopy reveals that the sub-wavelength pores (the smallest size ~ 100 nm) were generated by rapid solvent evaporation. The effect of pore size on water repellency and transparency of the prepared honeycomb-patterned films is discussed.

Copolymer **1**,[23] having equimolar amounts of fluorinated acrylate and methyl methacrylate monomers, was kindly provided by Asahi Glass Co., Japan (Chart 1, molecular weight = 39 000, T_g = 50.1 °C). For the experiments, the copolymer was dissolved in a fluorinated solvent (AK-225, a mixture of $CF_3CF_2CHCl_2$/$CClF_2CHClF$, Asahi Glass Co., Japan) at a concentration of 1.5 mg/mL.

A glass substrate (76 mm × 26 mm) was cleaned by UV−ozone treatment for 30 min (Ai ozone cleaner, Iwasaki Denki, Japan) and ethanol. Immersion in a 2 wt % AK-225 solution of 1*H*,1*H*,2*H*,2*H*-perfluorooctylchlorosilane for 30 min gave a fluorinated surface. To complete the surface modification, the glass substrate was baked at 120 °C for 2 h in an electric oven.

The fluorinated glass substrate was fixed to a moving substrate holder,[21] which was smoothly controlled by a computer-driven system (Figure 1). A metal blade was fixed perpendicular to the substrate, and the gap between the blade edge and the substrate was adjusted to about 100 μm. Fifty microliters of the fluorinated copolymer solution was cast on the substrate, and the substrate was moved in a straight line at 2 mm/s. The fluorinated copolymer solution was supplied to the gap between the blade and substrate. Then, humid air (relative humidity ~ 60% at room temperature) was applied to the solution surface with a flow velocity of 10 L/min. The formation of the honeycomb-patterned film was observed by an optical microscope (BH2, Olympus, Japan) and video recording system (DSR-30, Sony, Japan).

After evaporation of the solvent, the surface structure of the film was observed by a field-emission scanning electron microscope (FE-SEM, S-5200, Hitachi, Japan). The water contact angle on the honeycomb-patterned film was measured using a contact angle analyzer (G-1, ERMA, Japan). Ten microliters of membrane-filtered water was droppered onto the honeycomb-patterned films. The transmittance of the honeycomb-patterned films was measured using UV−vis spectroscopy (Lambda S900, Perkin-Elmer, Germany). The surface area fraction of pore and polymer was calculated from the SEM images of prepared films by using an imaging soft, NIH image (National Institute of Health, U.S.A.).

The formation of microporous structure essentially consists of four steps: (1) condensation of water droplets at the solution surface, (2) growth of the water droplets, (3) packing of the water droplets by capillary forces, and (4) complete evaporation of the solvent and subsequent evaporation of the water droplets.[17] Because the pores are formed based on the condensed water droplets as templates, size control of the condensed water droplets is important for regulation of the pore size. To produce a smaller pore size, the condensed water droplets should be small. We have previously reported that the pore size of honeycomb-patterned films can be controlled by the solvent evaporation time under a continuous supply of humid air. A larger application of casting solution gives a larger pore size for the honeycomb-patterned film. Consequently, immediate evaporation of the solvent is required to produce small pores.

To shorten the evaporation time, we reduce the thickness of the casting solution applied. In fact, the solvent evaporates immediately when the casting solution is spread as a homogeneous thin liquid film. For this purpose we have developed a simple device for supply of the polymer solution to the solid substrate as a thin liquid film (Figure 1). The solid substrate is fixed to a substrate holder that is moved horizontally. For application of the casting solution, a metal blade is fixed perpendicular to the substrate and the distance between the blade edge and the substrate surface is adjusted to less than 100 μm. Fifty microliters of polymer solution is cast on one side of the metal blade, and then the substrate is moved directly to the left side in Figure 1. As a result, the polymer solution is supplied as a thin liquid film from the narrow gap between the metal blade and the substrate.

The wettability of the substrate surface is important for the stability of the thin liquid film. Because the polymer and solvent are fluorinated in this experiment, the solution does not spread on a hydrophilic glass substrate, as a result of its low surface tension. Therefore, we modified the glass substrate using a fluorinated silane coupling agent. After modification, the contact angle of the fluorinated solvent on the substrate decreased to less than 10° and the solution spread homogeneously. By moving the substrate, the thin liquid film was applied while under a flow of humid air. The solvent immediately evaporated within one video frame (about 30 ms) as observed by the microscope.

Figure 2 shows FE-SEM images of the surface of the prepared film. On the front edge of the film, a random distribution of pores of varying size was observed. The pore size ranged from about 20 to 200 nm. The smallest pore size observed is comparable to the smallest theoretical size of a condensed water droplet at room temperature, 10 nm.[24] In contrast, at around 100 μm from the film edge, there is a regular arrangement of 100 nm pores. The pore size gradually increases to 300 nm with increasing distance from the film

(21) (a) Karthaus, O.; Cieren, X.; Maruyama, N.; Shimomura, M. *Mater. Sci. Eng. C* **1999**, *10*, 103. (b) Yabu, H.; Shimomura, M. *Int. J. Nanosci.* **2002**, *1* (5−6), 673.
(22) Shimomura, M.; Yabu, H.; Yamamoto, H.; Kaida, Y. Japanese Patent JP2005-023122, 2005.
(23) Yabu, H.; Shimomura, M. *Adv. Funct. Mater.* **2005**, *15* (4), 575.
(24) Kittel, C.; Kroemer, H. *Thermal Physics*; W. H. Freeman and Company: New York, 1980.

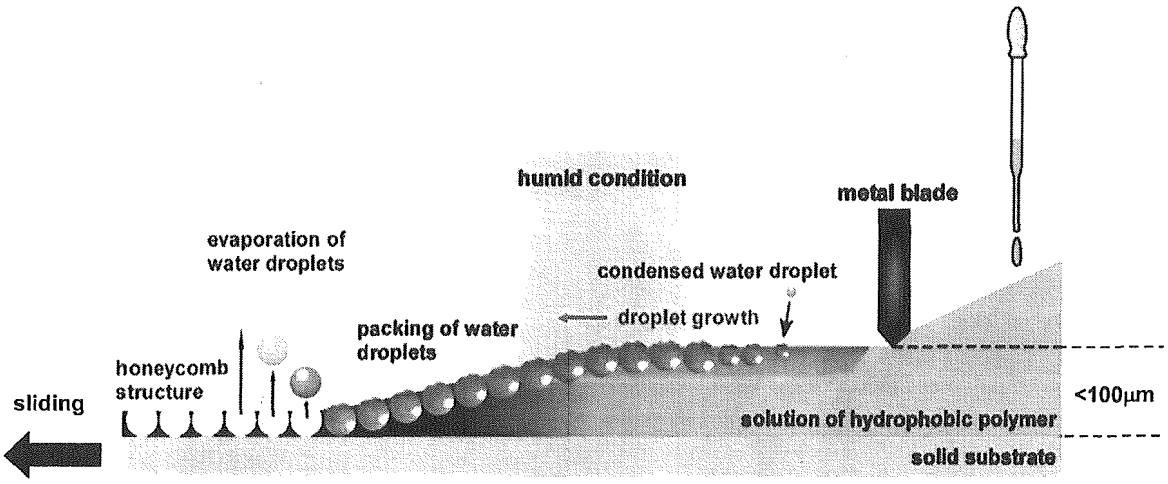

Figure 1. Schematic illustration of honeycomb-patterned film preparation.

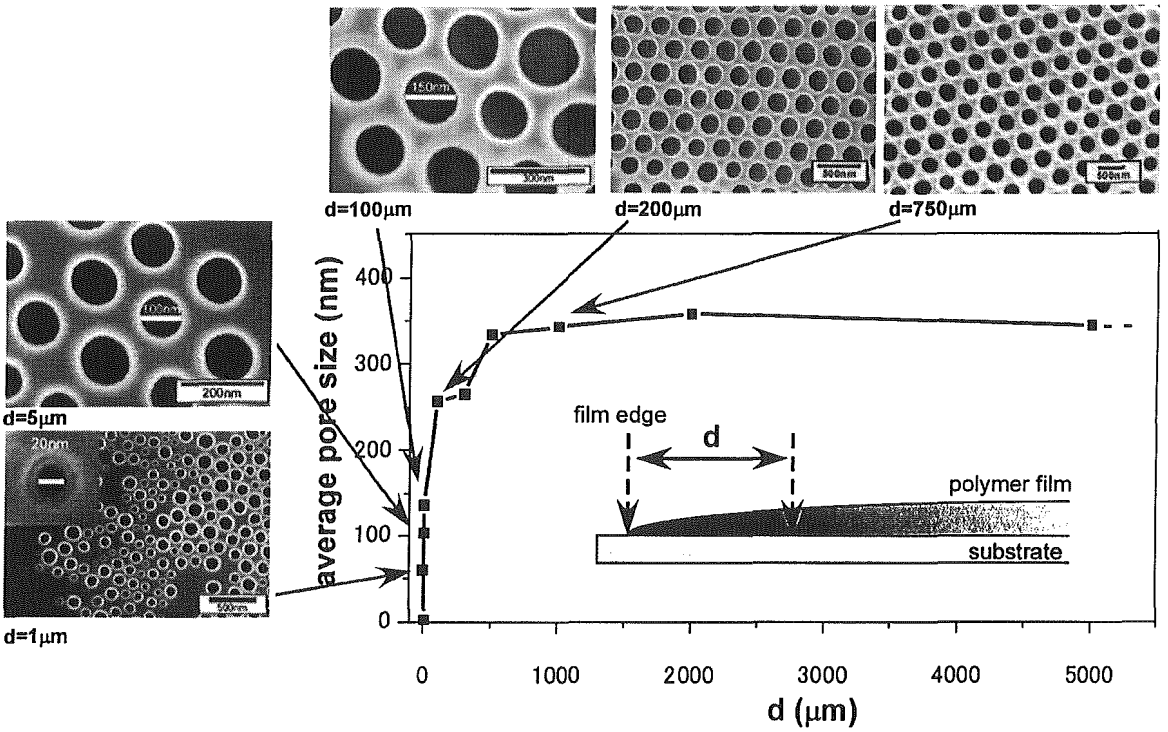

Figure 2. Plot of the average pore sizes and the distance from the film edge (*d*). FE-SEM images of the film surface taken on the different distances from the edge.

edge. Thus, under the described preparation conditions (humidity, temperature, moving speed), the pore size over the major part of the film was 300 nm.

Figure 2 indicates that the water droplet grows during their arrangement toward well-hexagonal packing. Thus, there is a tradeoff between reduction of the pore size and regular packing of the pores. In our case, the fast solvent evaporation rate applied to reduce the water droplet size seems to be balanced with a suitable time duration for regular arrangement of the condensed water droplets. The pore size of the honeycomb structure can be easily controlled up to 5 μm by changing the thickness of the liquid film from 100 μm to 1 mm.

We have previously reported that the water contact angle increases with decreasing pore size of the honeycomb-patterned fluorinated polymer.[25] The water contact angle on honeycomb-patterned films with 300 nm pores was measured to be 160° (Figure 3a). The sub-wavelength structure enhances the hydrophobicity of rough surfaces. This value is higher than that of a 2-μm-pore honeycomb-patterned film (145°). This value is also higher than the theoretical value. The theoretical contact angle on the honeycomb-patterned film of 300-nm-sized pores was calculated by using Cassie's law. From the calculation of the surface area fraction of the polymer part by using imaging software, the fraction of the polymer part was 0.20−0.26. By using Cassie's equation, the theoretical water contact angle on the honeycomb-patterned film with 300 nm pores was up to about 153° (see Supporting Information). The high contact angle measured on the honeycomb-patterned film is due to the surface

(25) Yabu, H.; Takebayashi, M.; Tanaka, M.; Shimomura, M. *Langmuir* **2005**, *21* (9), 3235.

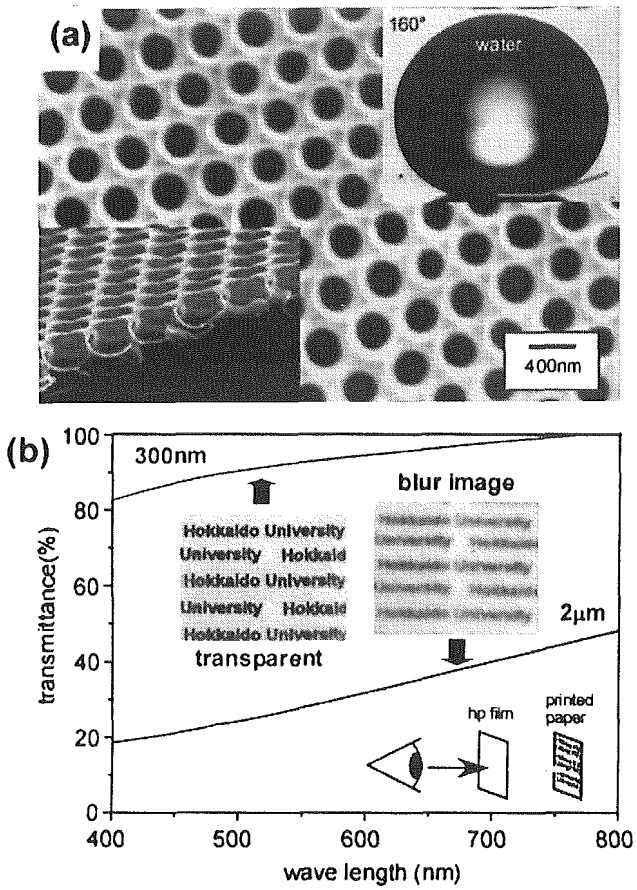

Figure 3. (a) Scanning electron micrograph of the 300-nm-sized honeycomb-patterned film (top image and cross section) and the water contact angle on this film. (b) Transmittance of the 2-μm- and the 300-nm-sized honeycomb-patterned films and photograph of the film with printed papers underneath.

roughness of the rim of honeycomb pores (see the cross section of the film in the inset of Figure 3a). The vertex of hexagons is slightly higher than the other part of the rim. Thus, the real contact area is smaller than the calculated value from the top image.

Transmittances of the micrometer (2 μm) and sub-wavelength (300 nm) honeycomb-patterned films were measured by UV−vis spectroscopy. Figure 3b clearly indicates that the transmittance of the 2-μm-pore film is lower than 50% whereas that of the submicrometer-sized honeycomb-patterned film is higher than 80%. The 2-μm-pore film is opaque, blurring the letters beneath the film (inset photograph in Figure 3b). On the other hand, the 300-nm-pore film is transparent enough to read the letters clearly through the film. It is also noted that the depths of the pores are also smaller than the visible wavelength (see cross-section image in Figure 3a). Thus, the film with 300 nm pores does not scatter light regardless of the incident light angles.

A simple method of preparing sub-wavelength-pore honeycomb-patterned films is demonstrated by casting of the polymer solution under humid conditions. By utilizing a specialized coating instrument we have developed, the thickness of the liquid film was reduced to less than 100 μm. The sub-wavelength honeycomb-patterned films obtained are optically transparent and exhibit superhydrophobicity. The smallest pore size was 20 nm. Our method does not require expensive techniques such as chemical vapor deposition, etching, or UV exposure. Further, the films can be formed from a large variety of materials and on a wide variety of substrates. Such sub-wavelength honeycomb-patterned films have application as transparent and superhydrophobic polymer films.

Acknowledgment. We thank Dr. H. Yamamoto and Dr. Y. Kaida for providing the fluorinated polymers. This work was partly supported by Grant-in-aid for scientific research, MEXT, Japan.

Supporting Information Available: Calculation of the theoretical contact angle by Cassie's law. This material is available free of charge via the Internet at http://pubs.acs.org.

CM051281I

Superhydrophobic and Lipophobic Properties of Self-Organized Honeycomb and Pincushion Structures

Hiroshi Yabu,*,†,‡ Masafumi Takebayashi,§ Masaru Tanaka,|| and Masatsugu Shimomura†,‡,⊥

Nanotechnology Research Center, Research Institute for Electronic Science, Hokkaido University, N21W10, Sapporo, 001-0021, Japan, Frontier Research System, Institute of Physical and Chemical Research (RIKEN Institute), 1-12, Hirosawa, Wako, Saitama, 351-0198, Japan, Core Research for Evolutional Science and Technology (CREST), Japan Science and Technology Agency (JST), 4-1-8, Honcho, Kawaguchi, Saitama, 332-0012, Japan, Graduate School of Science, Hokkaido University, N10W8, Sapporo, 060-0810, Japan, and Core Research Initiative "Sousei", Hokkaido University, N21W10, Sapporo, 001-0021, Japan

Received January 3, 2005. In Final Form: February 18, 2005

This report describes the simple preparation of superhydrophobic and lipophobic surfaces by self-organization. Microporous polymer films of a fluorinated polymer with hexagonally arranged pores were prepared by casting from solution under humid conditions. Hexagonally packed water microdroplets were formed by evaporative cooling on the surface of the casting solution. After solvent evaporation, a honeycomb-patterned polymer film was formed with the water droplet array acting as a template; the water droplets themselves evaporated soon after the solvent. Two porous polymer layers were stacked vertically, separated by pillars at the hexagon vertexes. After peeling off the top layer using adhesive tape, a pincushion-like structure was obtained. Here, we show that superhydrophobic behavior was achieved, with the maximum contact angle, 170°, observed using these pincushion structures. Theoretical calculations fit the experimental results well. The lipophobic properties of the films are also discussed.

1. Introduction

Surface wettability is a significant factor in determining the physical and chemical properties of materials. Superhydrophobic and lipophobic surfaces have found application in a variety of settings, including self-cleaning surfaces, prevention of snow sticking, oxidation and heat conduction processes, and others.[1−3] Considering the water repellency of plant leaves[4] as an example from nature, it is known that the chemical properties of the surface and its topology play important roles: waxy compounds secreted on the surface make the leaves hydrophobic, and surface roughness caused by the many small waxy bumps enhances this hydrophobicity. Fluorocarbon compounds, because of their low surface free energies,[5] are usually used to make the surfaces of materials water- or oil-repellent. To enhance the hydrophobicity of fluorocarbon surfaces, rough, microstructured surfaces have been prepared. Recent developments in photolithography techniques have enabled an investigation into the effect of surface topology on surface wettability.[6] A number of reports have described preparing superhydrophobic surfaces by using a fractal structure of wax,[7] chemical vapor deposition (CVD) of poly(tetrafluoroethylene) (PTFE),[8] and carbon nanotubes and walls[9] and by coating hydrophobic silanes onto sublimated aluminum acetylactonate.[10] These microstructured surfaces show a decrease in apparent surface free energies.[11] In this report, we describe the simple preparation of super water- and oil-repellent surfaces by self-organization.

2. Experimental Section

The fluorinated copolymer **1**, having equimolar amounts of fluorinated and methyl methacrylate repeat units, used in this experiment was kindly provided by Asahi Glass Co. (M_n = 39 000, n:m = 50:50, T_g = 50.1 °C), Japan. This copolymer was dissolved in AK-225 (a mixture of $CF_3CF_2CHCl_2$/$CClF_2CHClF$, Asahi Glass Co., Japan) at a concentration of 10 g/L. In all cases, ca. 20 μL to 5 mL of homogeneous solutions of **1** were dropped onto glass substrates at ambient temperature, with humid air (relative humidity, 40−60%) applied by an air pump (current velocity, 80−200 mL/min; a photograph of the experimental setup is available in the Supporting Information) to form honeycomb-patterned films. The pincushion structures were prepared by peeling off the tops of the honeycomb films using Scotch tape. The adhesive tape was stuck firmly to the film surface, after which the tape with the adhering top layer was separated from

* To whom correspondence should be addressed. Tel & Fax: +81-11-706-9369. E-mail: yabu@poly.es.hokudai.ac.jp.

† Nanotechnology Research Center, Research Institute for Electronic Science, Hokkaido University.

‡ Frontier Research System, Institute of Physical and Chemical Research (RIKEN Institute).

§ Graduate School of Science, Hokkaido University.

|| Core Research Initiative "Sousei", Hokkaido University

⊥ Core Research for Evolutional Science and Technology (CREST), Japan Scince and Technology Agency (JST).

(1) Ball, P. *Nature* **1999**, *400*, 507.

(2) Nakajima, A.; Watanabe, T. *Monatsh. Chem.* **2001**, *132*, 31.

(3) Gu, Z.-Z.; Uetsuka, H.; Takahashi, K.; Nakajima, R.; Onishi, H.; Fujishima, A.; Sato, O. *Angew. Chem., Int. Ed.* **2003**, *42* (8), 894.

(4) (a) Barthlott, W.; Neinhuis, C. *Planta* **1997**, *202*, 1. (b) Otten, A.; Herminghaus, S. *Langmuir* **2004**, *20* (6), 2405.

(5) Hozumi, A.; Takai, O. *Thin Solid Films* **1997**, *303*, 222.

(6) (a) Yoshmitsu, Z.; Nakajima, A.; Watanabe, T.; Hashimoto, K. *Langmuir* **2002**, *18* (15), 5818. (b) Miwa, M.; Nakajima, A.; Fujishima, A.; Hashimoto, K.; Watanabe T. *Langmuir* **2000**, *16* (13), 5754.

(7) Onoda, T.; Satoh, N.; Tsujii, K. *Langmuir* **1996**, *12* (9), 2125.

(8) (a) Chen, W.; Fadeev, A. F.; Hsieh, M. C.; Oner, D.; Youngblood, J.; McCarthy, T. J. *Langmuir* **1999**, *15* (10), 3395. (b) Bico, J.; Marzorin, C.; Quere, D. *Europhys. Lett.* **1999**, *47* (2), 220. (c) Öner, D.; McCarthy, T. J. *Langmuir* **2000**, *16* (20), 7777.

(9) (a) Li, H.; Wang, X.; Song, Y.; Liu, Y.; Li, Q.; Jiang, L.; Zhu, D. *Angew. Chem., Int. Ed.* **2003**, *40* (9), 1743. (b) Li, S.; Li, H.; Wang, X.; Song, Y.; Liu, Y.; Jiang, L.; Zhu, D. *J. Phys. Chem. B* **2002**, *106*, 9274. (c) Feng, L.; Li, S.; Li, Y.; Li, H.; Zhang, L.; Zhai, J.; Song, Y.; Liu, B.; Zhu, D. *Adv. Mater.* **2002**, *14* (24), 1857.

(10) Nakajima, A.; Fujishima, A.; Hashimoto, K.; Watanabe, T. *Adv. Mater.* **1999**, *11* (16), 1365.

(11) Wenzel, R. N. *Ind. Eng. Chem.* **1936**, *28*, 988.

10.1021/la050013w CCC: $30.25
Published on Web 03/08/2005

Chart 1

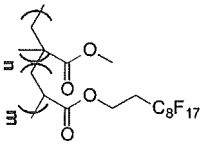

the bottom layer, which remained on the substrate. The pincushion structures were analyzed in the same manner as the honeycomb films.

The surface morphologies of the films were observed by optical microscopy (BH-2, Olympus, Japan), atomic force microscopy (AFM, SPI-400, Seiko Instruments, Japan), and scanning electron microscopy (SEM, S-3500N, Hitachi, Japan). The sizes of the prepared structures (pore size (d), rim width (r), pin height (h), pin width (w)) were measured from these micrographs using NIH Image software (this software can be freely obtained from the National Institutes of Health (NIH), U.S.A.). Gray scale SEM images were converted to monochrome. Contact angles of water and benzene on the prepared films were measured using a contact angle analyzer (G-1, ERMA Inc., Japan) as follows: a 5 μL liquid droplet was gently placed onto the films, and contact angles were measured 30 s after placement by the $\theta/2$ method. As a control experiment, a flat film was prepared by spin-coating the 10 g/L polymer solution at 1000 rpm onto a glass substrate.

3. Results and Discussion

It has been reported that microporous polymer films with hexagonally arranged pores can be cast from solution under humid conditions.[12-17] Hexagonally packed water microdroplets are formed by evaporative cooling on the surface of the casting solution, and these water droplets are transferred to the solution front by convectional flow or capillary force. When the water droplets condense on the solution surface, the clear solution turns opaque. After solvent evaporation, a honeycomb-patterned polymer film is formed with the water droplet array acting as a template; the water droplets themselves evaporate soon after the solvent.

By using this method, we have demonstrated the first fabrication of honeycomb-patterned films from fluorinated copolymers (**1**, Chart 1). A typical SEM image of the honeycomb-patterned film of **1** is shown in Figure 1a, in which hexagonally arranged micropores can be observed. The cross-section of the film is also shown in Figure 1a. The spherical shape of the pores reflects the shape of the template water droplets.[15] Two porous polymer layers were stacked vertically, separated by pillars at the hexagon vertexes. After peeling off the top layer using adhesive tape (Figure 1b), a pincushion-like structure was obtained (Figure 1c). Each pillar was broken into two sharp pins, one on the surface of each layer, after peeling.

The sizes of the honeycomb and pincushion structures were easily controlled by varying the casting volume of polymer solution. The pore size of the honeycomb-patterned films depended on the size of the template water droplets, and this in turn was dominated by the solvent evaporation time, which is equal to the water condensation time.[18] The pore size (d) and rim width (r) of honeycomb-

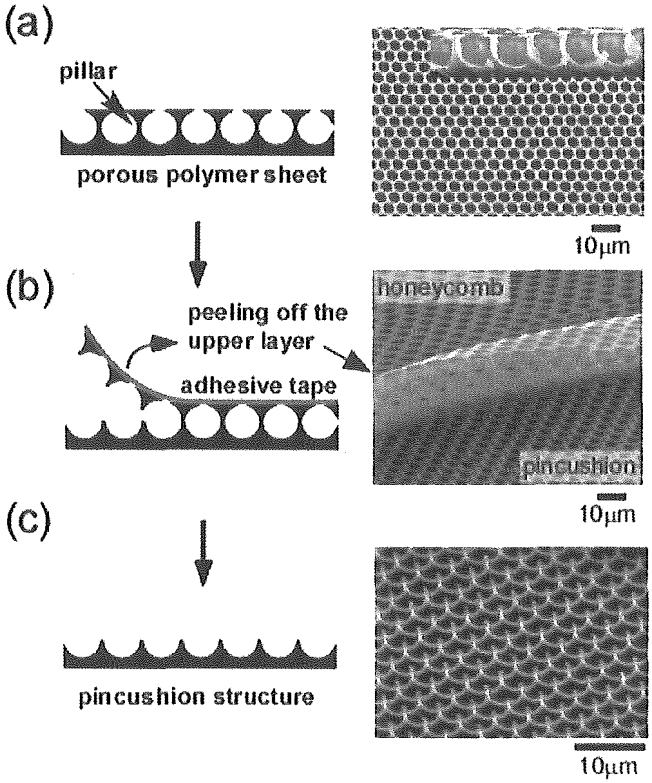

Figure 1. Schematic illustration and scanning electron micrograph of (a) the honeycomb-patterned film, (b) the peeling process, and (c) the pincushion structure.

patterned films were measured from each SEM image using NIH Image (Figure 2a). The average pore size and rim width of the films increased with increasing amount of polymer solution cast. The average pore size ranged from 490 nm to 5.5 μm by changing the casting volume from 20 μL to 7.5 mL, respectively. The width of the pins (w) likewise increased from 90 to 420 nm, respectively, corresponding to changes in the original honeycomb film (Figure 2b). The height of the pins (h) increased with increasing pore size, and dimple-like structures were formed when the pore size was small (d < 750 nm, inset of Figure 2b).

A superhydrophobic surface is defined as having a water contact angle of over 150°. The water contact angle of a flat film of **1** was 117°. This angle is higher than those of flat surfaces in materials containing hydrocarbon groups. For the honeycomb-structured film of **1**, the contact angle increased dramatically (Figure 2c) and depended on pore size. Superhydrophobic behavior was achieved by the pincushion structures, with the maximum contact angle, 170°, observed for pincushion structures prepared from honeycomb films with 1.6 μm pores. The contact angle of water increased with decreasing pin width. In the case of the dimple structures, the contact angle decreased to 140° because its topology was very similar to that of the honeycomb structure. As a result, the water contact angles on the dimpled and honeycomb-patterned films were also quite similar.

The water repellency of rough hydrophobic surfaces has been discussed for several decades. The superficial contact angle of a surface composed of two components (e.g., air and polymer) is given by a formula reported by Cassie and Baxter[19] based on the fraction of each component's

(12) Widawski, G.; Rawiso, M.; Francois, B. *Nature* **1994**, *369*, 397.
(13) Jenekhe, S. A.; Chen, X. L. *Science* **1999**, *283*, 372.
(14) Yonezawa, T.; Onoue, S.; Kimizuka, N. *Adv. Mater.* **2001**, *13*, 140.
(15) (a) Maruyama, N.; Koito, T.; Nishida, J.; Sawadaishi, T.; Cieren, X.; Ijiro, K.; Karthaus, O.; Shimomura, M. *Thin Solid Films* **1998**, *327*, 854. (b) Karthaus, O.; Maruyama, N.; Cieren, X.; Shimomura, M.; Hasegawa, H.; Hashimoto, T. *Langmuir* **2000**, *16* (15), 6071. (c) Yabu, H.; Tanaka, M.; Ijiro, K.; Shimomura, M. *Langmuir* **2003**, *19* (15) 6297.
(16) Pitois, O.; Francois, B. *Eur. Phys. J. B* **1999**, *8*, 225.
(17) Govor, L. V.; Bashmakov, I. A.; Kaputski, F. N.; Pientka, M.; Parisi, J. *Macromol. Chem. Phys.* **2000**, *201*, 2721.
(18) (a) Beysens, D.; Knobler, C. M. *Phys. Rev. Lett.* **1986**, *57* (12), 1433. (b) Beysens, D. *Atmos. Res.* **1995**, *39*, 215, (c) Limaye, A. V.; Narhe, R. D.; Dhote, A. M.; Ogale, S. B. *Phys. Rev. Lett.* **1996**, *76* (20), 3762.

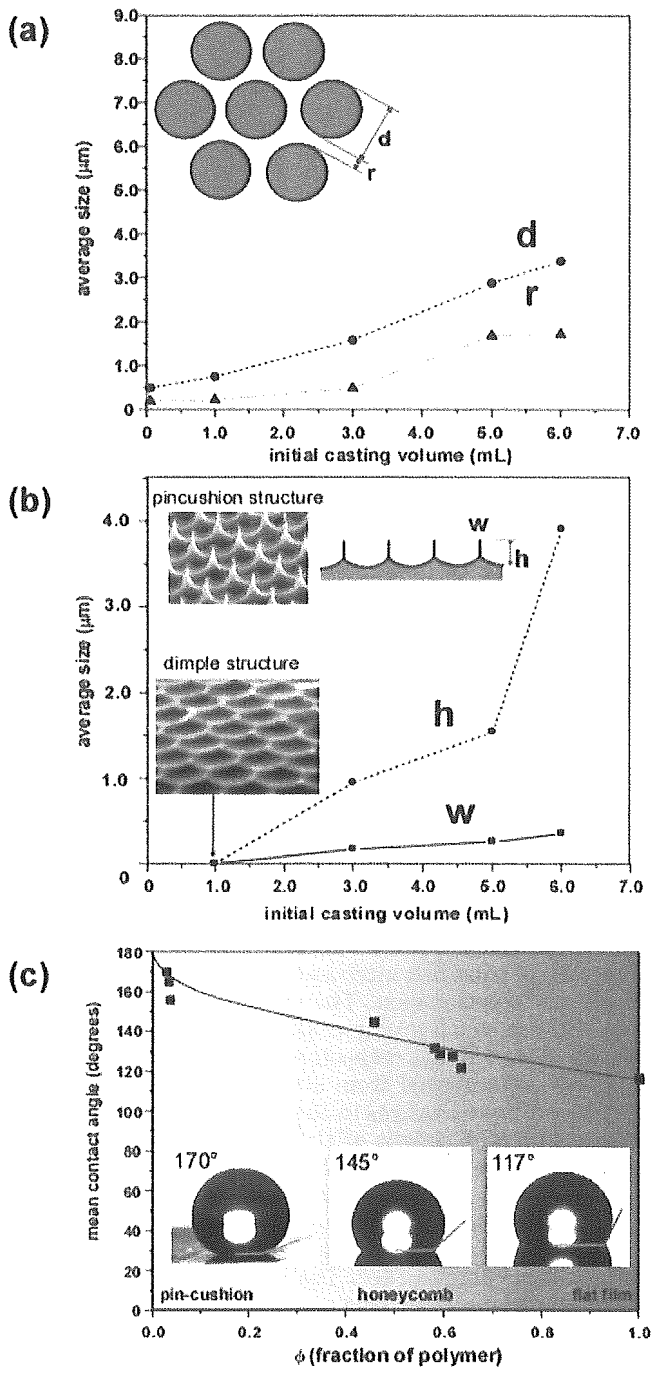

Figure 2. The size change of honeycomb structures and pincushion structures. (a) Pore diameter (d) and rim width (r) of honeycomb structures. (b) The size change of pin height (h) and width. (c) Water contact angles on different ϕ_1 surfaces. The black dots and the line indicate experimental and calculated results, respectively.

surface area. According to Cassie's law,

$$\cos \theta_c = \phi_1 \cos \theta_1 + \phi_2 \cos \theta_2 \quad (1)$$

where θ_c is the superficial contact angle; θ_1 and θ_2 are contact angles of flat films of components 1 and 2, respectively; and ϕ_1 and ϕ_2 are surface area fractions of polymer and air, respectively. When component 2 is air, $\cos \theta_2$ is -1, and ϕ_2 equals $(1 - \phi_1)$. Equation 1 then becomes

$$\cos \theta_c = \phi_1(\cos \theta_1 + 1) - 1 \quad (2)$$

The surface area fraction of the polymer (ϕ_1) was calculated from the size of these structures. For the pincushion structures, this fraction only took into account the tops of the pins. The ϕ_1 values of the honeycomb and pincushion structures were 0.46–0.64 and 0.028–0.043, respectively. According to eq 2, a large air void is required to achieve a high contact angle. The calculated ideal contact angle for each ϕ_1 is shown as a black line in Figure 2c, which indicates that the theoretical calculations fit the experimental results well. That the experimental results were not perfectly matched in the pincushion regime may have been due to nonuniformity of the pin structures from stress applied during peeling.

Another important advantage of fluorocarbon materials is their lipophobicity arising from their low surface free energies. Since it was expected that certain surface topologies would enhance lipophobicity as well as hydrophobicity, the contact angles of the lipophilic solvent benzene were also measured on the honeycomb and pincushion films. This contact angle was higher on the pincushion structure than on the honeycomb-patterned films. The highest contact angle of benzene measured in this experiment was 135°. There are few lipophobic materials having contact angles higher than 100°, because benzene has a low surface tension of 28.9 dyn/cm at 20 °C (compared to 73 dyn/cm for water). The benzene contact angle of the dimple structure was low for the same reason as that for the water case.

4. Conclusion

This report describes the preparation of superhydrophobic and lipophobic surfaces from fluorinated polymers by a water-assisted self-organization process. A honeycomb-patterned film was prepared by casting a fluorinated polymer solution on a solid substrate under humid conditions. After peeling off the top layer of the honeycomb structure, a pincushion structure was formed. The films showed superhydrophobic and lipophobic properties. Our method has some advantages over other reported methods: (1) this method can be used for large scale production of superhydrophobic coatings, (2) this method can be applied to a wide variety of hydrophobic polymers, and (3) this method provides a new low-cost fabrication process, with low energy consumption. These superhydrophobic and lipophobic films can be utilized for dust-free, low-friction coatings.

Acknowledgment. We thank Dr. Hirotsugu Yamamoto and Dr. Yuriko Kaida for kindly providing us with the fluorinated copolymer. This work is partly supported by a Grant-in-Aid for Scientific Research, MEXT, Japan.

Supporting Information Available: Experimental setup for preparation of honeycomb-patterned films; photo of a benzene droplet placed on the pincusion structure prepared from peeling the top layer of a honeycomb-patterned film. This material is available free of charge via the Internet at http://pubs.acs.org.

LA050013W

(19) Cassie, A. B. D. *Discuss. Faraday Soc.* **1948**, *3*, 11.

Zinc dental fillings and palmoplantar pustulosis

Teruki Yanagi, Tadamichi Shimizu, Riichiro Abe and Hiroshi Shimizu

Lancet 2005; 366: 1050

Department of Dermatology (T Yanagi MD, T Shimizu MD, R Abe MD, H Shimizu MD), **Hokkaido University Graduate School of Medicine, N15W7, Kita-ku, Sapporo 060-8638, Japan**

Correspondence to:
Dr Teruki Yanagi
yanagi@med.hokudai.ac.jp

In January, 2005, a 59-year-old Japanese woman was referred to our hospital with a 5-week history of inflammatory skin lesions on her palms and soles. Physical examination revealed multiple pustules, vesicles, and scaly erythema disseminated over her palms and soles; clinically, the signs were typical of palmoplantar pustulosis (PPP) (figure). Laboratory data and complete blood counts were within normal limits. She had no tonsillitis and a pharyngeal culture test was negative. Detailed medical history revealed that the patient had received extensive treatment for dental caries with dental metal restorations for five teeth 1 year earlier. We suspected a possible relation between the PPP and dental metal allergy. To see whether there was any metal allergy, we did patch testing on her forearm with the metal standard patch test series (Torii Pharmaceutical Co, Ltd, Tokyo, Japan), including aluminium chloride, chromium sulphate, cobalt chloride, copper sulphate, ferric chloride, gold chloride, indium trichloride, iridium tetrachloride, manganese chloride, mercury bichloride, nickel sulphate, platinum chloride, palladium chloride, potassium dichloride, stannous chloride, silver bromide, and zinc chloride. After 48 h there was a pronounced positive reaction with zinc; all other tests were negative. Severe exudative erythema with multiple pustules, clinically similar to PPP, appeared in the patch test area resulting from zinc chloride 2% petrolatum (figure, inset). Skin biopsy of the test site showed sterile, intraepidermal pustules, pathologically identical to PPP. Furthermore, drug lymphocyte stimulating tests (DLST) revealed a very strong reaction to zinc sulphate with stimulating index 1880% (normal <180%). Analysis of her dental filling showed that it contained gold, indium, silver, palladium, copper, tin, and zinc.

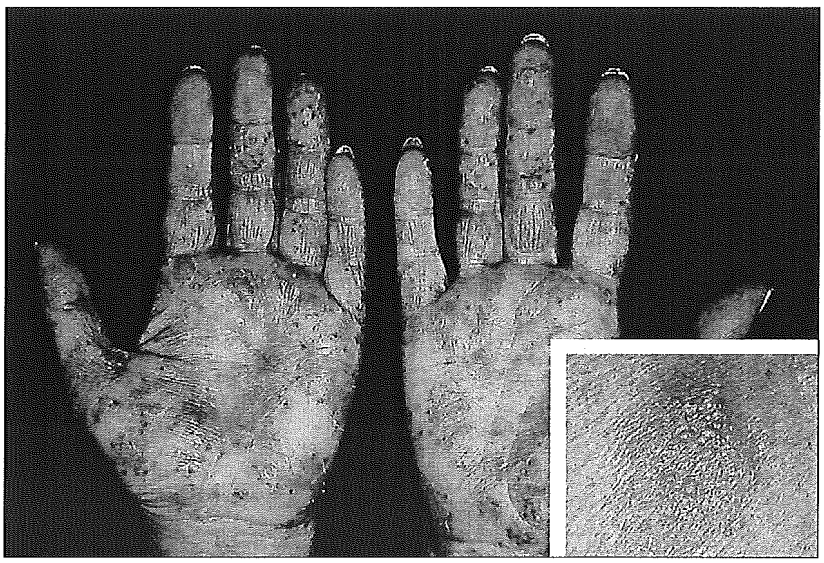

Figure: **Palmoplantar pustulosis showing pustules, vesicles, and scaly erythema**
Inset: pustule formation, clinically equivalent to PPP, was observed over the zinc chloride patch test area (after 48 h).

On the basis of clinical history, positive patch test with characteristic histology, and positive DLST index, we concluded that the patient's PPP was induced by zinc allergy. Therefore, all her dental fillings were completely removed and changed to a zinc-free compound. Although no oral or topical medication was given, the patient's PPP showed an improvement soon after the removal of the fillings, and complete cure was achieved in only 4 weeks. When last seen in July, 2005, the patient was well and there has been no sign of recurrence.

PPP is a chronic skin disease characterised by sterile intraepidermal pustules associated with erythematous scaling on the palms and soles.[1] Although the cause of PPP is not completely known, association with thyroid disease, smoking, and focal infections, such as tonsillitis, has been suggested.[1,2] Recently, metal allergy associated with PPP, including nickel, iron, and cobalt, has been reported.[3] Here we report zinc-allergy-induced PPP in which histologically identical pustules were produced by zinc patch test, and a complete remission was subsequently achieved by removal of zinc dental restorations. The relation between PPP and metal allergy has been reported in the Japanese population, but this has not been widely recognised elsewhere.[3,4]

References

1 Eriksson MO, Hagforsen E, Lundin IP, Michaelsson G. Palmoplantar pustulosis: a clinical and immunohistological study. *Br J Dermatol* 1998; 138: 390–98.

2 Akiyama T, Seishima M, Watanabe H, Nakatani A, Mori S, Kitajima Y. The relationships of onset and exacerbation of pustulosis palmaris et plantaris to smoking and focal infections. *J Dermatol* 1995; 22: 930–34.

3 Nakamura K, Imakado S, Takizawa M, et al. Exacerbation of pustulosis palmaris et plantaris after topical application of metals accompanied by elevated levels of leukotriene B4 in pustules. *J Am Acad Dermatol* 2000; 42: 1021–25.

4 Nakayama H, Nogi N, Kasahara N, Matsuo S. Allergen control. An indispensable treatment for allergic contact dermatitis. *Dermatol Clin* 1990; 8: 197–204.

Relationship between adsorbed fibronectin and cell adhesion on a honeycomb-patterned film

Sadaaki Yamamoto [1,2,*], Masaru Tanaka [1,2], Hiroshi Sunami [1,2], Keiko Arai [3], Aiko Takayama [2], Shigeko Yamashita [2], Yuka Morita [1], Masatsugu Shimomura [2, 3, 4]

1.Creative Research Initiative "Sousei" (CRIS), Hokkaido University, N21W10 Kita-ku, Sapporo 001-0021, Japan, 2. Core Research for Evolutional Science and Technology(CREST), Japan Science and Technology Agency (JST), Honchou 4-1-8, Kawaguchi 332-0012, Japan, 3. Spatio-Temporal Function Materials Research Group, Frontier Research System[3], RIKEN Institute, 1-12 Hirosawa, Wako. Saitama 351-0198, Japan, 4.Nanotechnology Research Center, Research Institute for Electronic Science, Hokkaido University[4], N12W6 Kita-ku, Sapporo 060-0812, Japan.

*Corresponding author. Tel:+81-11-706-9255, Fax:+81-11-706-9291; Email: syama@cris.hokudai.ac.jp

Abstract

Substratum surface morphology plays a vital roles in cellular behavior. Here, we characterized adsorption of fibronectin (Fn) as a typical cell adhesion protein onto honeycomb-patterned films made of poly(ε-caprolactone) (PCL) by using atomic force microscopy (AFM) and confocal laser scanning microscopy (CLSM). In oder to determine how cells adhere to a honeycomb-patterned film, focal adhesion of cardiac myocytes (CMYs) and endothelial cells (ECs) on the films were studied by using fluorescence labeling of vinculin. Fn adsorbs around the pore edges to form ring-shapes structures. CMYs and ECs adhere onto the honeycomb-patterned films at focal contact points localized around pore edges distributed over the entire cellular surface. The focal contact points on the honeycomb-patterned films correspond well with the adsorption sites of Fn. We suggest that the cell response to honeycomb-patterned films is associated with the adsorption pattern of Fn on the film.

Key words: Atomic force microscopy, Scanning electron microscopy, Cell adhesion, Adsorption, Self-assembly, Surface topography, Fibronectin, Tissue engineering

Introduction

Tissue engineering aims to restore, maintain, or improve complex human tissue function by using synthetic and living components [1]. Cells and the development of cytokines and scaffolds (cell-culture substrates) are key issues in tissue engineering. Since the original report that cells react to surfaces [2] , cell response to material surfaces has been an intriguing topic in tissue engineering. Extensive research has documented that surface properties such as chemistry, charge, rigidity, and topography play vital roles in cellular behavior, such as adhesion, spreading, migration, proliferation, and differentiation. Recently, cell culture substrates with geometric micro-and nano-patterns have been fabricated by various methods and have been extensively used to investigate how cells respond to surface topography [3-24]. Although the effects of nano- and micro-patterned topography on cell responses have been well documented, the mechanisms behind these effects remain unresolved.

Fibronectin (Fn) is representative of a class of important cell adhesion proteins that are found in blood and associated with cell surfaces [25]. When adsorbed onto biomaterials, Fn undergoes a conformational change from a globular structure to extended structure, depending on surface properties such as surface charge, hydrophobicity, hydrophilicity, and plays a critical role in mediating cell responses. To determine the role of Fn in mediating cell responses, adsorption of Fn both in molecularly isolated and aggregated states has been extensively investigated on various kinds of substrates, such as silica [26], methylated silica [26], mica [26,28] titanium [27], poly(metylmetacrylate) [28], sulfonated polystyrene [29], and glass [30] by using AFM, scanning electron microscopy (SEM), and fluorescence resonance energy transfer. Although adsorption of Fn is thus well-documented, little is known about the effect of substratum surface nano-and micro-pattern roughness on such adsorption [31].

Studies using biochemical methods suggest that structural changes in cell adhesion proteins such as fibronectin during adsorption onto a substrate determined by topography affect the molecular binding sites of these proteins to a receptor in cells, and thus affect the biological performance of these proteins and, ultimately, their critical role in mediating cell behavior [32,33]. Therefore, the correlation between the structures of adsorbed protein molecules and the substratum surface properties has been extensively researched. A detailed clarification of the effect of surface topography on protein adsorption requires a separation of the topographical and chemical effects, and, thus, requires a nano-

and microfabrication method to form geometrical patterns with no variation in surface chemical properties. We have previously reported that honeycomb-patterned porous polymer films can be prepared by simple casting of polymer solutions of a water-immiscible solvent under high humidity (about 80% relative humidity at 21±1℃) [11-13,21,34-36]. The pore size of the films can be controlled over a wide range, from hundreds of nanometers to hundreds of microns. By mechanical stretching a honeycomb-patterned film made of a viscoelastic polymer, pores of various shapes, such as hexagonal, elongated hexagonal, rectangular, square-like, or triangle-like, can be formed in a controlled way [24]. Our recent studies on the culture of cells, such as endothelial cells (EC), cardiac myocytes (CMYs), neural projenitor cells, and hepatocytes, on honeycomb-patterned films revealed that cellular behavior such as migration, spreading, and morphology can be controlled by the size and shape of pores of the film [11,13,19,21,24]. These characteristics of honeycomb-patterned films make these films suitable candidates for cell-culture substrates used in studying the effect of substratum surface morphology on the adsorption of adhesive proteins and the role that morphology plays in cell behavior.

On honeycomb-patterned films, the conformational change in adhesion protein molecules such as fibronectin required for focal contact adhesion is supposedly the mechanism behind this control. In this study, the effect of surface morphology on the structure of adsorbed Fn was assessed by using atomic force microscopy (AFM) and confocal laser scanning microscopy (CLSM). Further, in order to determine how cells adhere to a honeycomb-patterned film, focal adhesion of cardiac myocytes (CMYs) and endothelial cells (ECs) on the films were studied by using fluorescence labeling of vinculin. The results showed that the structure of adsorbed Fn depends on the surface morphology of the films. Based on the structure of adsorbed Fn, the focal contact points of both types of cells on a honeycomb-patterned film are probably determined by the structure of Fn, leading to the characteristic biological response of a honeycomb-patterned film different from that of a flat film.

Experimental Section

Materials

PCL and an amphiphilic copolymer (hereafter called Cap,) of dodecylamide and ω-carboxyhexylacrylamide were used in the film fabrication. PCL (Wako) has a molecular weight of 70,000-100,000. Cap was synthesized by a method previously reported [37]. Fn was a bovine plasma fibronectin (lyophilized from 0.05M

tris-buffer saline, pH7.5) purchased from Sigma. Water was purified using a Millipore system (Milli-Q, Millipore). Benzene, chloroform, and 10% formalin solution (Wako) were used without further purification.

Film Preparation

Honeycomb-patterned porous films (hereafter called honeycomb films) were fabricated on cover glasses (φ=15mm, Matsunami Glass Industry, Japan) by a method previously reported [24,34-36].

Adsorbed Fn assay

The quantity of adsorbed Fn onto the films was determined for different coating concentrations using bicinconic acid (BCA) as protein assay reagent (Pierce, IL) [29]. Different concentrations of Fn (0-1000 μg/ml) were adsorbed in 24-well tissue culture plates (Iwaki, Japan) for 24 h at 37 ℃ in 5% CO_2. The Fn solutions were removed from the plates, and then the films were washed two times in PBS. The reaction started at 37 ℃ after working reagent at 200 μl/well was added. After incubation for 2 h, 160 μl of the Fn solution was transferred into a 96-well plate for reading by a microplate reader (BiotrakII, Biochrom Ltd., U.K.) at the 590-nm wavelength.

AFM, CLSM, and SEM measurements

Tapping-mode AFM imaging was performed under ambient conditions using a Digital Instrument Nanoscope IIIa Multimode system (Digital Instrument, Santa Barbara CA) equipped with silicon nitride tips. The tips had a resonance frequency of ~300 kHz and a force constant of 14 N/m. The scan rate was 0.1-0.2 Hz, and the proportional and integral gains were set in the range of 2-10. CLSM measurements were performed using a CLSM apparatus (FLUOVIEW FV300, Olympus). The SEM images were obtained using a Hitachi S-3500N SEM (Hitachi, Japan) at an acceleration voltage of 15 kV. A 200-μl aliquot of 240 μg/ml bovine plasma Fn (Sigma, Munich Germany) in phosphate-buffered saline (PBS) was added to each honeycomb film and then incubated at 37 ℃ in 5% CO_2. The Fn-coated films were then gently washed with PBS, fixed with 10% formaldehyde (Wako) for 10 min at room temperature, permeabilized in PBS containing 1% normal goat serum and 0.1 % Triton X-100 for 30 min., and then the film was incubated for 1 h with anti-Fn antibody (diluted 1:500; Sigma). After being rinsed with water, the films were treated with fluoresein isothiocyanate (FITC)-conjugated anti-rabbit IgG antibody (diluted 1:2000). The specimens for SEM were sputter-coated with Au-Pd using a sputter-coating unit (Hitachi E1030, Hitachi, Japan).

Cell Culturing

CMYs were isolated by enzyme treatment of minced heart tissues of 19-day rat embryos (Sprague Dawley rats, Japan SLC, Inc) [38]. CMYs were seeded onto the pre-fabricated cell-culture substrates (i.e., a flat film and a self-supported honeycomb film) at a density of 1.0×10^5 cells/cm^2. Culture medium pre-warmed at 37 ℃ (Hepes-buffered Hams F10 containing 0.5% ITS and 3% FCS) was replaced daily. One day and three days after seeding, vinculin of CMYs was stained as follows. Cells were fixed by immersion in 4% paraformaldehyde (SIGMA) solution for 10min and permeabilized by immersion in 0.1% Triton X-100 (SIGMA) solution for 10 min. Cells were incubated for 1.5 h with mouse monoclonal anti vinculin IgG_1 antibodies (CHEMICON international, Inc) in 10% blocking solution (Dainippon Sumitomo Pharma) at 37 ℃. After washing with PBS, vinculin complex were visualized by incubation with Alexa Fluor 488 anti-mouse IgG antibodies (Molecular Probe) for 1 h at 37 ℃.

Porcine aortic endothelial cells (ECs, CSC Certificate ™ DAINIPPON PHARMACEUTICAL CO. LTD) were purchased. After the frozen cells were thawed at 45℃, they were resuspended into a culture medium (Duibecco's Modified Eagle's Medium, SIGMA) containing 10% FBS, 100 unit/ml penicillin, and 100 μg/ml streptomycin. A honeycomb film and a flat film on glass plates were preincubated in the culture medium for 72 h at 37 ℃ in 5% CO_2 before cell seeding. ECs (passage number of 6-8) were seeded on the films at a density of 1.5×10^4 cells/cm^2. Culture medium was replaced after days 1, 3, 5, and 7. To visualize the focal adhesion, vinculin was stained by using an immunological method with primary antibodies (diluted 1:100, CHEMICON) and fluorescence-labeled secondary antibodies (diluted 1;1000, Alexa Fluor 546 goat anti-mouse IgG, Molecular Probes). For immunostaining, cells were fixed by immersion in 10% formalin (Wako) at 20 ℃ for 10 min and permeated with 1% PBS solution of Triton X-100 for 5 min at 20 ℃.

Results and Discussion

Figure 1 shows SEM images of the structure of the PCL honeycomb film. The top-view image (Fig.1a) reveals a well-arranged hexagonal lattice. The side-view image (Fig.1c) reveals that the honeycomb films were porous with a double-layered structure in which two hexagonal lattices were connected vertically by pillars at the vertex of hexagons. A schematic model of this double-layered structure is shown in Fig. 1d.

The amount of Fn adsorbed on both the flat and honeycomb films was measured as a function of incubation time and of Fn-coating concentration

determined by using a total adsorbed protein assay. The amount of Fn adsorbed on both films increased linearly with incubation time up to 1 h, and then became saturated . With increasing Fn-coating concentration up to 50 μg/ml, Fn adsorption on the flat film increased drastically and then saturated when the Fn-coating concentration reached 600 μg/ml. Although the adsorption behavior on the honeycomb films was similar to that on the flat films, the amount of Fn adsorbed on the honeycomb films was twice that on the same size of flat films. Considering the three-dimensional porous structure of the honeycomb films (Fig.1), the higher amount of adsorbed Fn might be due to the larger surface area of the film. This possibility is supported by the depth profile of the fluorescence intensity from stained Fn obtained by scanning excitation laser light from top to bottom of the films in CLSM. In the depth profile, fluorescence was observed only at the top and bottom surfaces of the honeycomb films and not within the film (data not shown), suggesting that Fn adsorbed onto the top (front and rear sides of the top layer) and bottom layer of a honeycomb film. Because the ratio of pore area to total surface area (porosity) of a top sheet is about 0.5, the estimated surface area of a honeycomb film for Fn adsorption is about twice that of a flat film, and thus the amount of Fn adsorbed on a honeycomb film should be about twice that on a flat film. The amount of adsorbed Fn at saturation on a flat film was 0.52 μg and that on a honeycomb film was 0.91 μg. The surface density at saturation on a flat film calculated using the surface area of a flat film (1.32 cm^2) and the adsorbed amount (0.52 μg) was about 0.4 $\mu g/cm^2$. This value agrees well with the approximate amount of Fn required for monolayer coverage, namely, 0.32 $\mu g/cm^2$, based on reported estimates of the dimension of a Fn molecule [32,33,39,40]. Based on the estimated surface area of a honeycomb film (twice the surface area of a flat film), the surface density of Fn on a honeycomb film is equal to that on a flat film. The total adsorbed protein assay revealed a monolayer-level adsorption behavior of Fn on both the flat and honeycomb films.

Figure 2a shows AFM images of the surface of a flat film at 48 h incubation in 240 μg/ml Fn/PBS solution at 25 ℃. Despite the monolayer-level adsorption, the surface was not uniform but had an interconnected fibrillar structure. Typical fibrils reached 30-50 μm in length, 0.5-2 μm in width, and 0.05-0.2 μm in height (AFM image shown in Fig. 2b). The CLSM image of stained Fn adsorbed on the flat films revealed a fibrillar structure similar to that revealed by AFM (Fig.2c). Both images indicate that Fn adsorbs on the flat films to form aggregates with a fibrillar structure, similar to that of Fn adsorbed onto sulfonated polystyrene films [29],

supporting our assignment that the fibril-like aggregates are adsorbed Fn.

Both CLSM and AFM images reveal that adsorption structure of Fn on a honeycomb film depend on incubation time up to 48 h (Fig. 3). Both images show that the surface of the honeycomb film after incubation in Fn/PBS solution completely differs from that of a flat film and depends on the incubation time. At an incubation time of 0 h, the surface is flat. At 24 h incubation, distinctly different morphologies coexist on the surface (AFM image in Fig. 3a); the surface above the dashed line in Fig.3a is covered by numerous globules, whereas the surface below the dashed line is uniform. The distribution of the fluorescence from stained Fn in the CSLM image corresponds well to the morphological differences observed in the AFM image (Fig. 3b). By 48 h incubation, a few globules remain, and ring structures about 100 nm high and 1 μm wide appear around the pores as a dominant structure. Several rings were scraped off while repeating the tip scanning (as shown by white arrows in Fig. 3c). The CLSM image (Fig. 3d) reveals strong ring-like fluorescence along the pore edges, corresponding well to the ring structures evident in the AFM images. AFM image (Fig. 3e) reveals that the surface of the honeycomb films incubated in PBS solution between 0 and 48 h without Fn is uniform, and shows no evidence of any adsorbates. Both AFM and CLSM images reveal that Fn adsorbed and underwent a structural transition from globular form on the rim of the film to ring form around the edges of pores. A similar time-dependent self-organization of Fn has been reported for adsorption of Fn onto a sulfonated polystyrene surface [29], although the amount of adsorbed Fn was much higher than that for the honeycomb films used in our study.

The amount of adsorbed Fn on both films remains relatively constant, regardless of incubation time (longer than 1 h). Furthermore, the morphologies of the aggregates depend on the substrate surface structure (note that the chemical composition of both the honeycomb films and flat films was the same). Because protein molecules bound to a surface can rearrange via conformational changes [41] and diffusion [42], three-dimensional aggregate formation is possible, even for molecules adsorbed irreversibly with random orientations without overlapping or closed-packed monolayer density [43]. The structural transition from globular form to fibrillar form can be ascribed to the self-organization of adsorbed Fn caused by the dependence of diffusion on the surface morphology (honeycomb pattern and flat surface). Protein organization on a patterned surface has been reported for Fn adsorption onto Au/Si micropatterns coated by a sulfonated polystyrene film [31]. Fn was adsorbed on the Si regions of the substrate but was repulsed by the Au

domains, resulting in a structure of self-assembling Fn determined by the width of Si domains. The possible mechanism behind this Fn organization on the patterned surface is the balance between the bending energy of Fn and the unfavorable energy of contact with the Au interface. In our current study, the width of a rim of a honeycomb film on which Fn adsorbed was about 5 μm. The width of a rim and the size of a pore are comparable to the width of Si and Au domains of Au/Si micropatterns (several microns to 20 microns). If pores play a role similar to the role that Au domains play, namely, that Fn does not adsorb, the same mechanism might be responsible for the self-organization of Fn on a honeycomb film.

To determine how cells adhere to a honeycomb film, vinculin within focal adhesions and actin cytoskeleton linked to integrin receptor in cell membranes were examined here by using immunofluorescence staining (Fig. 4). The focal contact points on a flat film clearly depend on the cells; EC adheres onto a flat film at cell peripheries and focal adhesions are very faint, whereas the focal contact points of CMYs are located randomly over entire cell bodies and the focal adhesions are strongly evident. Focal adhesion differs significantly between the honeycomb films and flat film. On the honeycomb films, focal adhesions of both types of cells are distributed over the entire cellular surface and located around the edges of pores lying beneath the cell bodies. Focal adhesion formation and subsequent actin polymerization are essential to a cell's ability to adhere. Integrin receptors recognize a specifically distinct peptide sequence of Fn (cell-binding RGD integrin recognition motif) that mediates cell-substrate focal contact adhesion. Binding of adhesion receptors to adsorbed Fn provides mechanical coupling to the underlying substrate and activates signal transductive pathways that control cellular behavior such as proliferation and differentiation [44]. The location of focal contact points corresponds well with the adsorption sites of Fn, suggesting that the focal adhesion pattern on honeycomb films is determined by the adsorption pattern of Fn. Focal contact points are regularly aligned on the honeycomb films. This adhesion pattern implies that the distance between adjacent focal contact points and/or the density of focal contact points are determined precisely by the pore size, and this distance and/or density might play a vital role in activating the signal transductive pathways. This control of focal contact points by the pore size might be an origin of the pore-size dependence of cell response characteristics to a honeycomb film.

Summary

In this study, the adsorption structure of Fn and the adhesion patterns of ECs and CMYs on honeycomb films and flat films was studied, and the role the honeycomb film plays on cell response were discussed. Results showed that the structure of adsorbed Fn was determined by the micro-pattern pores of the honeycomb film and by incubation time. The structure of adsorbed Fn changed with increasing incubation time from globular to fibril-like form. The fibril-like aggregates were located on the periphery of micro-pores. The focal contacts of the cells located on the periphery of the micro-pores are apparently determined by the fibril-like form of adsorbed Fn. We suggest that the cell response to the honeycomb-patterned film is associated with the ordered adsorption pattern of Fn on the honeycomb film, leading to the characteristic response of a honeycomb film different from that of a flat film. The results presented here suggest a mechanism where the structure of the adsorbed cell adhesion proteins determined by a substrate micro-pattern affects the molecular binding sites of the proteins to a receptor in cells, affects the biological performance of the proteins and, thus ultimately affects their critical role in mediating cell behavior.

Acknowledgements

This study was supported by a Special Coordination Funds for Promoting Science and Technology, Ministry of Education, Culture, Sports, Science and Technology, Japan (Mext), CREST-JST (Grants-in-Aid from the Japan Science and Technology Corporation)

References

[1] R. Langer and J. P. Vacanti, Science, 260 (1993) 920.

[2] A. Carrel and M. Burrows, J. Exp. Med. 13 (1911) 571.

[3] J. A. Hubbel, Bio/Technology 13 (1996) 565.

[4] C. S. Chen, M. Mrksich, S. Huang, G. M. Whitesides and D. E. Ingber, Science, 276 (1997) 1425.

[5] A. M. Green, J. A. Jansen, J-P. C. M. van der Waerden and A. F. von Recum, J. Biomed. Mater. Res. 28 (1994) 647.

[6] S. Turner, L. Kam, M. Isaacson, H. G. Graighead, W. Shain and J. Turner, J. Vac. Sci. Technol. 15 (1997) 2848.

[7] A. Curtis and C. Wilkinson, Biomaterials, 18 (1997) 1573.

[8] R. S. Kane, S. Takayama, E. Ostuni, D. E. Ingber and C. M. Whiteside, Biomaterials, 20 (1999) 2363.

[9] E. T. den Braber, J. E. de Reijter, L. A.Ginsel, A. F. van Recum and J. A. Jansen, J. Biomed. Mater. Res. 40 (1998) 291.

[10] A. Folch and M. Toner, Biotechnol. 14 (1998) 388.

[11] T. Nishikawa, J. Nishida, R. Ookura, S. Nishimura, S. Wada, T. Karino and M. Shimomura, Mater. Sci. Eng. C8-9 (1999) 495.

[12] T. Nishikawa, J. Nishida, R. Ookura, S. Nishimura, S. Wada, T. Karino and M. Shimomura, Mater. Sci. Eng. C10 (1999) 141

[13] K. Sato, K. Hasebe, M. Tanaka, M. Takebayashi, K. Nischikawa, M. Schimomura, T. Kawai, M. Matsushita and S. Todo, Int. J. Nanosci. 1 (2002) 689.

[14] H. G. Graighead, C. D. James and A. M. P. Turner, Curr. Opi. Sol. State Mater. Sci. 5 (2001) 177.

[15] A. Mata, C. Boehm, A. J. Fleischman, G. Muschlar and S. Roy, J. Biomed. Mater. Res. 62 (2002) 499.

[16] M. Arnold, A. E. Cavalcanti-Adam, R. Glass, J. Blümmel, W. Eck, M. Kantlehner, H. Kessler and J. P. Spatz, ChemPhysChem 5 (2004) 383.

[17] X. F. Walboomers, L. A. Ginsel and J. A. Jansen, J. Biomed. Mater. Res, 51 (2000) 529.

[18] N. M. Dowell-Mesfin, M-A. Abdul-Karim, A. M. P. Turner, S. Scanz, H. G. Craighesd, B. Roysam, J. N. Turner and W. Shain, J. Neural Eng. 1 (2004) 78

[19] A. Tsuruma, M. Tanaka, N. Fukushima and M. Shimomura, e-J. Surf. Sci. Nanotech. 3 (2005) 159.

[20] M. J. Dalby, M. O. Riehle, D. S. Sutherland, H. Agheli and A. S. G. Gurtis, J. Biomed. Mater. Res 69A (2004) 314.

[21] T. Nishikawa, J. Nishida, R. Ookura, H. Ookubo, H. Kamachi, M. Matsushita, S. Todo and M. Schimomura, Stud. Surf. Sci. Catl. 132 (2001) 132, 509.

[22] F. A. Denis, P. Hanarp, D. S. Sutherland, J. Gold, C. Mustin, P. G. Rouxhet and Y. F. Dufrêne, Langmuir 18 (2002) 819.

[23] M. J. Dalby, S. Childs, M. O. Riehle, H. J. H. Johnstone, S. Affrossman and A. S. G. Curtis, Biomaterials, 24 (2003) 927.

[24] T. Nishikawa, M. Nonomura, K. Arai, J. Hayashi, T. Sawadaishi, Y. Nishiura, M. Hara and M. Shimomura, Langmuir, 19 (2003) 6193.

[25] R. O. Hynes, Fibronectin, (New York, Springer 1990) p546.

[26] M. Bergkvist, J. Carlsson and S. Oscarsson, J. Biomed. Mater. Res. 64A (2003) 349.

[27] D. E. MacDonald, B. Markovic and M. Allen, J. Biomed. Mater. Res. 41 (1998) 120.

[28] E. R. Zenhausen, M. Jobin, M. Taborelli and P. Descounts, Ultramicroscopy, 42-44(Pt B) (1992) 1155.

[29] N. Pernodet, M. Rafailovich, J. Sokolov, D. Xu, N-L.Yamg and K. J. McLeod, Biomed. Mater. Res. 64A (2003) 684.

[30] L. Bough and V. Vogel, J. Biomed. Mater. Res. 69 (2004) 525.

[31] N. Pernodet, S. Lenny, J. John and R. Miriam, American Phys. Soc., March Meeting 2004, March 22-26, 2004,Palais des Congress de Montreal, Montreal, Quebec, Canada, Meeting ID; MAR04, abstract#P9.011

[32] A.G. Garcia, M. D. Vega and D. Boettinger, Mol. Biol. Cell, 10 (1999) 785.

[33] A. G. Garcia and D. Boettinger, Biomaterials, 20 (1999) 2427.

[34] N. Maruyama, T. Koito, J. Nishida, T. Sawadaishi, X. Gieren, K. Ijiro, O. Karthaus and M. Shimomura, Thin Solid Films, 854 (1998) 327.

[35] T. Nishikawa, R. Okura, J. Nishida, K. Arai, J. Hayashi, N. Kurono, T. Sawadaishi, M. Hara and M. Schimomura, Langmuir 18 (2002) 5734.

[36] M. Tanaka, M. Takebayashi, M. Miyama, J. Nishida and M. Schimomura, Bio-Med. Mater. Eng. 14 (2004) 439.

[37] S. Nishimura and K. Yamada, J. Am. Chem. Soc. 119 (1997) 10555.

[38] M. C. Denyer, M. Riehle, M. Scholl, C. Sproessler, S. T. Britland, A. Offenhaeusser and W. Knoll, In Vitro Cell. Dev. Biol. Anim. 35 (1999) 352.

[39] F. Grinnel and M. K. Feld, J. Biomed. Mater. Res. 15 (1981) 363.

[40] E. C. Williams, P. A. Janmey, J. D. Ferry and D. F. Mosher,; J. Biol. Chem. 257 (1982) 14973.

[41] W. G. Pitt, S. H. Spiegelberg and S. L. Cooer, in: Proteins at interfaces Physicochemical and Biochemical Studies (J. L. Brash and T. A. Horbett). ACS Symposium series, p.324. Amer. Chem. Soc. Washinton, DC,1987.

[42] R. D. Tilton, C. R. Robertson and A. P. Gast, J. Colloid Interface Sci.137 (1990) 192.
[43] P. A. Dimilla, S. M. Albelda and J. A. Quinn, J. Collid Interface Sci. 153 (1992) 212.
[44] K. Buridge and M. Charanowska-Wodnick, Ann. Rev. Cell Dev. Biol. 12 (1996) 463